

World Journal of *Stem Cells*

World J Stem Cells 2024 March 26; 16(3): 228-323



EDITORIAL

- 228 O-linked β -N-acetylglucosaminylation may be a key regulatory factor in promoting osteogenic differentiation of bone marrow mesenchymal stromal cells
Zhou XC, Ni GX
- 232 Understanding host-graft crosstalk for predicting the outcome of stem cell transplantation
Labusca L, Zugun-Eloae F
- 237 High glucose microenvironment and human mesenchymal stem cell behavior
Mateen MA, Alaagib N, Haider KH

MINIREVIEWS

- 245 How mesenchymal stem cells transform into adipocytes: Overview of the current understanding of adipogenic differentiation
Liu SS, Fang X, Wen X, Liu JS, Alip M, Sun T, Wang YY, Chen HW

ORIGINAL ARTICLE**Retrospective Study**

- 257 Long-term outcome of stem cell transplantation with and without anti-tumor necrotic factor therapy in perianal fistula with Crohn's disease
Park MY, Yoon YS, Park JH, Lee JL, Yu CS

Basic Study

- 267 Low-intensity pulsed ultrasound reduces alveolar bone resorption during orthodontic treatment *via* Lamin A/C-Yes-associated protein axis in stem cells
Wu T, Zheng F, Tang HY, Li HZ, Cui XY, Ding S, Liu D, Li CY, Jiang JH, Yang RL
- 287 Self-assembly of differentiated dental pulp stem cells facilitates spheroid human dental organoid formation and prevascularization
Liu F, Xiao J, Chen LH, Pan YY, Tian JZ, Zhang ZR, Bai XC
- 305 Evaluation of genetic response of mesenchymal stem cells to nanosecond pulsed electric fields by whole transcriptome sequencing
Lin JJ, Ning T, Jia SC, Li KJ, Huang YC, Liu Q, Lin JH, Zhang XT

ABOUT COVER

Editorial Board Member of *World Journal of Stem Cells*, Yu-Hong Li, PhD, Associate Professor, Department of Cell Biology, Army Medical University, Chongqing 400038, China. liyuhongtmmu@hotmail.com

AIMS AND SCOPE

The primary aim of *World Journal of Stem Cells (WJSC, World J Stem Cells)* is to provide scholars and readers from various fields of stem cells with a platform to publish high-quality basic and clinical research articles and communicate their research findings online. *WJSC* publishes articles reporting research results obtained in the field of stem cell biology and regenerative medicine, related to the wide range of stem cells including embryonic stem cells, germline stem cells, tissue-specific stem cells, adult stem cells, mesenchymal stromal cells, induced pluripotent stem cells, embryonal carcinoma stem cells, hemangioblasts, lymphoid progenitor cells, *etc.*

INDEXING/ABSTRACTING

The *WJSC* is now abstracted and indexed in Science Citation Index Expanded (SCIE, also known as SciSearch®), Journal Citation Reports/Science Edition, PubMed, PubMed Central, Scopus, Biological Abstracts, BIOSIS Previews, Reference Citation Analysis, China Science and Technology Journal Database, and Superstar Journals Database. The 2023 Edition of Journal Citation Reports® cites the 2022 impact factor (IF) for *WJSC* as 4.1; IF without journal self cites: 3.9; 5-year IF: 4.5; Journal Citation Indicator: 0.53; Ranking: 15 among 29 journals in cell and tissue engineering; Quartile category: Q3; Ranking: 99 among 191 journals in cell biology; and Quartile category: Q3. The *WJSC*'s CiteScore for 2022 is 8.0 and Scopus CiteScore rank 2022: Histology is 9/57; Genetics is 68/325; Genetics (clinical) is 19/90; Molecular Biology is 119/380; Cell Biology is 95/274.

RESPONSIBLE EDITORS FOR THIS ISSUE

Production Editor: Xiang-Di Zhang; Production Department Director: Xu Guo; Cover Editor: Jia-Ru Fan.

NAME OF JOURNAL

World Journal of Stem Cells

ISSN

ISSN 1948-0210 (online)

LAUNCH DATE

December 31, 2009

FREQUENCY

Monthly

EDITORS-IN-CHIEF

Shengwen Calvin Li, Carlo Ventura

EDITORIAL BOARD MEMBERS

<https://www.wjgnet.com/1948-0210/editorialboard.htm>

PUBLICATION DATE

March 26, 2024

COPYRIGHT

© 2024 Baishideng Publishing Group Inc

INSTRUCTIONS TO AUTHORS

<https://www.wjgnet.com/bpg/gerinfo/204>

GUIDELINES FOR ETHICS DOCUMENTS

<https://www.wjgnet.com/bpg/GerInfo/287>

GUIDELINES FOR NON-NATIVE SPEAKERS OF ENGLISH

<https://www.wjgnet.com/bpg/gerinfo/240>

PUBLICATION ETHICS

<https://www.wjgnet.com/bpg/GerInfo/288>

PUBLICATION MISCONDUCT

<https://www.wjgnet.com/bpg/gerinfo/208>

ARTICLE PROCESSING CHARGE

<https://www.wjgnet.com/bpg/gerinfo/242>

STEPS FOR SUBMITTING MANUSCRIPTS

<https://www.wjgnet.com/bpg/GerInfo/239>

ONLINE SUBMISSION

<https://www.f6publishing.com>

Basic Study

Self-assembly of differentiated dental pulp stem cells facilitates spheroid human dental organoid formation and prevascularization

Fei Liu, Jing Xiao, Lei-Hui Chen, Yu-Yue Pan, Jun-Zhang Tian, Zhi-Ren Zhang, Xiao-Chun Bai

Specialty type: Cell and tissue engineering**Provenance and peer review:** Unsolicited article; Externally peer reviewed.**Peer-review model:** Single blind**Peer-review report's scientific quality classification**Grade A (Excellent): A
Grade B (Very good): B
Grade C (Good): 0
Grade D (Fair): 0
Grade E (Poor): 0**P-Reviewer:** Cordelier P, France; Li SC, United States**Received:** December 19, 2023**Peer-review started:** December 19, 2023**First decision:** January 12, 2024**Revised:** January 21, 2024**Accepted:** February 28, 2024**Article in press:** February 28, 2024**Published online:** March 26, 2024**Fei Liu**, School of Basic Medical Sciences, Southern Medical University, Guangzhou 510515, Guangdong Province, China**Fei Liu, Jun-Zhang Tian**, Department of Health Management, Guangdong Second Provincial General Hospital, Guangzhou 510317, Guangdong Province, China**Jing Xiao**, Guangdong Provincial Key Laboratory of Tumor Interventional Diagnosis and Treatment, Zhuhai People's Hospital Affiliated with Jinan University, Zhuhai 519000, Guangdong Province, China**Jing Xiao**, Centre of Reproduction, Development and Aging, Faculty of Health Sciences, University of Macau, Macau 999078, China**Lei-Hui Chen, Yu-Yue Pan**, Department of Stomatology, Guangdong Second Provincial General Hospital, Guangzhou 510317, Guangdong Province, China**Zhi-Ren Zhang**, Zhuhai Institute of Translational Medicine, Zhuhai Hospital Affiliated with Jinan University, Zhuhai 519000, Guangdong Province, China**Xiao-Chun Bai**, Department of Cell Biology, School of Basic Medical Sciences, Southern Medical University, Guangzhou 510515, Guangdong Province, China**Corresponding author:** Xiao-Chun Bai, PhD, Professor, Department of Cell Biology, School of Basic Medical Sciences, Southern Medical University, No. 1023-1063 Shatai South Road, Baiyun District, Guangzhou 510515, Guangdong Province, China. baixc15@smu.edu.cn

Abstract

BACKGROUND

The self-assembly of solid organs from stem cells has the potential to greatly expand the applicability of regenerative medicine. Stem cells can self-organise into micro-sized organ units, partially modelling tissue function and regeneration. Dental pulp organoids have been used to recapitulate the processes of tooth development and related diseases. However, the lack of vasculature limits the utility of dental pulp organoids.

AIM

To improve survival and aid in recovery after stem cell transplantation, we demonstrated the three-dimensional (3D) self-assembly of adult stem cell-human dental pulp stem cells (hDPSCs) and endothelial cells (ECs) into a novel type of

spheroid-shaped dental pulp organoid *in vitro* under hypoxia and conditioned medium (CM).

METHODS

During culture, primary hDPSCs were induced to differentiate into ECs by exposing them to a hypoxic environment and CM. The hypoxic pretreated hDPSCs were then mixed with ECs at specific ratios and conditioned in a 3D environment to produce prevascularized dental pulp organoids. The biological characteristics of the organoids were analysed, and the regulatory pathways associated with angiogenesis were studied.

RESULTS

The combination of these two agents resulted in prevascularized human dental pulp organoids (Vorganoids) that more closely resembled dental pulp tissue in terms of morphology and function. Single-cell RNA sequencing of dental pulp tissue and RNA sequencing of Vorganoids were integrated to analyse key regulatory pathways associated with angiogenesis. The biomarkers forkhead box protein O1 and fibroblast growth factor 2 were identified to be involved in the regulation of Vorganoids.

CONCLUSION

In this innovative study, we effectively established an *in vitro* model of Vorganoids and used it to elucidate new mechanisms of angiogenesis during regeneration, facilitating the development of clinical treatment strategies.

Key Words: Human dental pulp stem cells; Prevascularized organoids; Integrated analyses; Angiogenesis; Forkhead box protein O1

©The Author(s) 2024. Published by Baishideng Publishing Group Inc. All rights reserved.

Core Tip: We demonstrated the three-dimensional self-assembly of adult stem cell-human dermal papilla cells and endothelial cells into a novel type of spheroid-shaped dental pulp organoid *in vitro* under hypoxia and conditioned medium. These organoids have been constructed to be morphologically and functionally closer to dental pulp tissue. Through the integration and analysis of single-cell RNA sequencing and RNA sequencing data, forkhead box protein O1 and fibroblast growth factor 2 were identified as crucial markers involved in the regulation of organoid angiogenesis. In this innovative study, we effectively established an *in vitro* model of prevascularized dental pulp organoids and used it to elucidate new mechanisms of angiogenesis during regeneration, facilitating the development of clinical treatment strategies.

Citation: Liu F, Xiao J, Chen LH, Pan YY, Tian JZ, Zhang ZR, Bai XC. Self-assembly of differentiated dental pulp stem cells facilitates spheroid human dental organoid formation and prevascularization. *World J Stem Cells* 2024; 16(3): 287-304

URL: <https://www.wjgnet.com/1948-0210/full/v16/i3/287.htm>

DOI: <https://dx.doi.org/10.4252/wjsc.v16.i3.287>

INTRODUCTION

The main experimental tool and goal of tissue regeneration engineering is the implantation of specific stem cells into diseased environments to repair and compensate for the dysfunction of damaged tissues and organs. However, the complexity and variability of the tissue microenvironment at the site of injury, such as hypoxic lethality, the inflammatory response, immune resistance and inadequate blood supply, leads to low survival rates (success rates of approximately 1%-3%) and poor maturation rates of directed differentiation after stem cell transplantation, all of which limit the clinical application and promotion of stem cells[1,2]. Therefore, it is critical for stem cells to form additional microvessels after implantation to quickly connect to the host's circulatory system and form functional blood vessels to ensure nutrient and oxygen delivery after implantation.

Organoids are constructed *in vitro* following an *in vivo* developmental programme that allows cells to grow, migrate, differentiate and function in three-dimensional (3D). A variety of organoids are currently constructed *in vitro*[3,4]. Compared to traditional 2D culture methods, 3D culture facilitates cell access to bio-factors and reduces intercellular shear force, which promotes the proliferation and differentiation of dental pulp stem cells. With the advent of 3D pulp culture technology, great progress has been made in regenerative endodontic procedures[5-7]. Although the construction of organoid models has outstanding advantages in terms of clinical application, it still faces a major challenge, namely, the lack of model nourishment due to the absence of angiogenesis, which is the main dilemma for the *in vitro* application of such models. In recent years, numerous studies have investigated the relationship between angiogenesis and pulp regeneration[7,8]. Several researchers have proposed that the addition of high concentrations of nutrients and their controlled and sustained release from scaffolds are important strategies for optimising angiogenesis during pulp regeneration[9]. A hydrogel scaffold was used in combination with conditioned media to release bio-factors in a controlled manner, which subsequently promoted blood vessel and nerve formation and dental tissue repair[10].

Our previous study revealed that hypoxia-activated phosphatidylinositol 3 kinase/protein kinase B (PI3K/Akt) inhibits oxidative stress in human dental pulp stem cells (hDPSCs) by regulating reactive oxygen species[11], thereby maintaining stem cell stemness during *in vitro* expansion. In addition, a number of signalling pathways associated with angiogenesis are activated, and the expression of regulatory factors associated with angiogenesis is altered. Does using hypoxic hDPSCs in *in vitro* organoid cultures better induce angiogenesis? How can prevascularized organoids be constructed to address current challenges in stem cell applications? Is angiogenesis regulated by the same mechanisms in dental pulp and prevascularized dental pulp organoids (Vorganoids)?

We induced endothelial cells (ECs) and hDPSCs in culture and subsequently fused the two cell types to obtain Vorganoids, which are morphologically and functionally more similar to dental pulp tissue. Single-cell RNA sequencing (scRNA-seq) of dental pulp tissue and RNA-seq of Vorganoids were subsequently integrated to analyse key regulatory pathways associated with angiogenesis in dental pulp tissue. Vascular endothelial growth factor A (VEGFA), a key signalling pathway regulating the differentiation of vascular ECs in dental pulp tissue, was also significantly enriched in the development of Vorganoids. The biomarkers forkhead box protein O1 (FOXO1) and fibroblast growth factor 2 (FGF2) were identified to be involved in the regulation of Vorganoids. In this innovative study, we effectively established an *in vitro* model of prevascularized dental pulp organoids and used it to elucidate new mechanisms of angiogenesis during regeneration, facilitating the development of clinical treatment strategies.

MATERIALS AND METHODS

Single-cell data download and preprocessing

We downloaded the GSE161266 dataset from the Gene Expression Omnibus database[12] and performed the following analyses: (1) Quality control and selection of cells for further analysis; (2) Background correction; (3) Selection of high-variability features (identification of high-variability markers in single-cell populations as candidate regulatory genes); (4) Dimensionality reduction (principal component analysis, linear dimensionality reduction, and determination of the appropriate “dimensionality” of the dataset); (5) Clustering of cell populations based on principal component analysis; and (6) Nonlinear dimensionality reduction by the UMAP/tSNE algorithm. Identification of differentially expressed genes (DEGs) in cell subpopulations. Dataset quality control was performed by removing cells with < 200 expressed genes, low-quality/dying cells, and empty droplets (cells with a mitochondrial genome accounting for > 5% of the total genome were selected)[13-15]. Subsequently, global scaling normalisation of overall expression was performed for the cells included in the analyses, and the expression levels were log-transformed. To reduce the noise in the data, Seurat’s nonlinear dimensionality reduction algorithm was used to extract the principal components of the core data regarding the “meta-features” of the clustered dataset. Based on the similarity of the cell expression profiles, cells were grouped into highly related subpopulations and clusters using the KNN algorithm[13,15].

Cell cluster definition and pseudotime-series analysis

Cell clusters were reannotated by the SingleR and scCATCH algorithms[14]. For the cell clusters with inconsistent annotation results, cell markers were visualised for analysis and determination of the cell subpopulation. Pseudotime-series analysis was performed on the entire cell population and core cell subpopulations. The Monocle algorithm was used to analyse the serial changes in gene expression experienced by each cell during the process of cell-state transition; this algorithm reveals the overall “trajectory” of gene expression changes and defines the appropriate regulatory point of each cell in the trajectory[16]. Based on the Monocle algorithm, cells were arranged in 2D space according to their global expression profiles, and the cell state trajectory was plotted. Subsequently, DEGs with kinetic correlations were identified by differential expression analysis based on the pseudotime values[13,15].

Functional enrichment analysis of the core cell subpopulations identified by pseudotime-series analysis

Based on the above analyses, core cell subpopulations were selected, and DEGs with kinetic correlations were subjected to pathway enrichment analysis: (1) The clusterProfiler package was used for Gene Ontology (GO) enrichment analysis (biological process, molecular function, and cellular component)[17]; and (2) GSEA was used to calculate the enrichment scores of pathways[18]: (1) Cell expression profiles were obtained from the preparation of samples for calculation of gene expression; (2) In preparation of the gene set, the core pathway gene list was downloaded from the MSIGDB database (<https://www.gsea-msigdb.org/gsea/msigdb/index.jsp>); and (3) The gene set was introduced into the algorithm, the pathways were scored by the GSEA algorithm for each sample, and the pathway scores were subjected to relative quantification.

RNA-seq analysis

The RNA-seq data units corresponding to the FPKM values of the samples were included. Differential gene expression analysis was performed on the samples from the two clusters with the most significant difference in survival. The DESeq algorithm was used to normalise the gene expression profiles and filter out genes with low expression[19]. The criteria for selecting DEGs were as follows: Log₂-fold change ≥ 1.5 and Benjamini-Hochberg (B-H) adjusted *P* value < 0.05. Through unsupervised cluster analysis, the identified DEGs were clustered according to the sample group, and GO enrichment analysis of these genes was subsequently performed to explore their potential biological functions through the ToppGene Suite (<https://toppgene.cchmc.org>)[20].

Gene functional enrichment analysis

Gene set enrichment analysis (GSEA) was performed to identify the core pathways and regulatory genes whose expression significantly changed. Further clustering and quantitative analysis of the core pathways and involved genes were performed using GSVA and the Ternary Cluster. Finally, regulatory genes related to pathological progression in the core cell subpopulations were obtained.

Cell culture and identification

The hDPSCs were collected from pulp tissues of extracted third molars from patients aged 18 to 25 years (12 males and 8 females). Cells from the first to fifth passages were used in this study. All patients were informed, agreed to participate in this study, and signed an informed consent. The study protocol was approved by the Ethics Committee of Guangdong Second Provincial General Hospital. Multiple differentiation assays for hDPSCs were performed according to a previously described procedure. Once the cells had reached 70%-80% confluence, the hDPSCs were allowed to differentiate in osteogenic, chondrogenic, or adipogenic induction media. The induction medium was changed every 2 d until the differentiated cells were harvested.

Analysis of cell surface markers

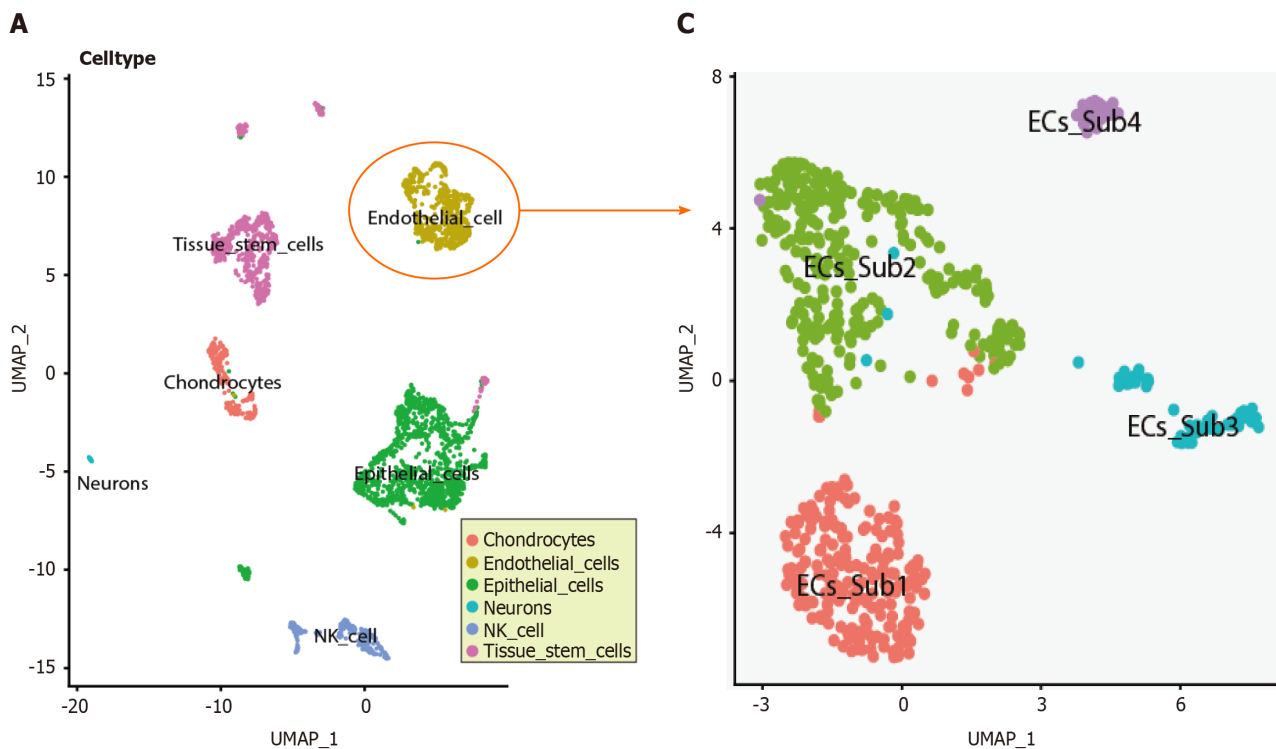
The hDPSCs were washed and resuspended in phosphate buffered saline (containing 1% foetal bovine serum) and then labelled with monoclonal anti-human CD146-PE, CD90-APC, CD34-PerCP and CD45-APC (Chemicon, Temecula, CA) for 30 min. The cells were washed twice, resuspended in staining buffer and analysed by flow cytometry.

Strategies for the construction of a model for the study of vascularized human dental pulp-like organs

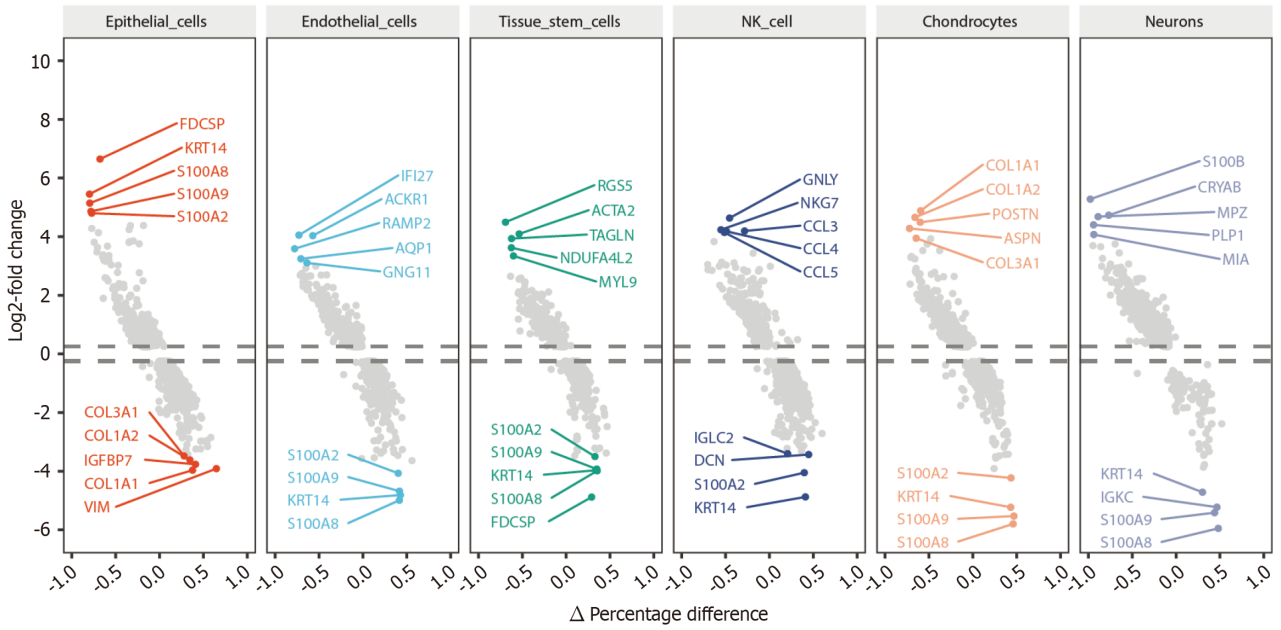
Preconditioning: Primary hDPSC cultures were incubated under 3% hypoxia beginning at passage 1. When the cells had expanded to passage 3, vasculogenic conditioned medium 1 (CM1) was added, and the culture was continued under hypoxic conditions for 7 d. CM1: EGM2 + 10% foetal bovine serum + 50 ng/mL VEGF 165 rh.

Aggregate formation: Hypoxic cells were then mixed with conditionally induced cells at a 2:8 ratio (total 5×10^4 cells) in a 96-well low-attachment plate containing 150 μ L of CM2 per well. CM2: CM1 + 50 μ M Y27632 + 5 μ L Matrigel. After 1 d of 3D culture, the medium was changed to CM1, and the incubation continued for 6 d.

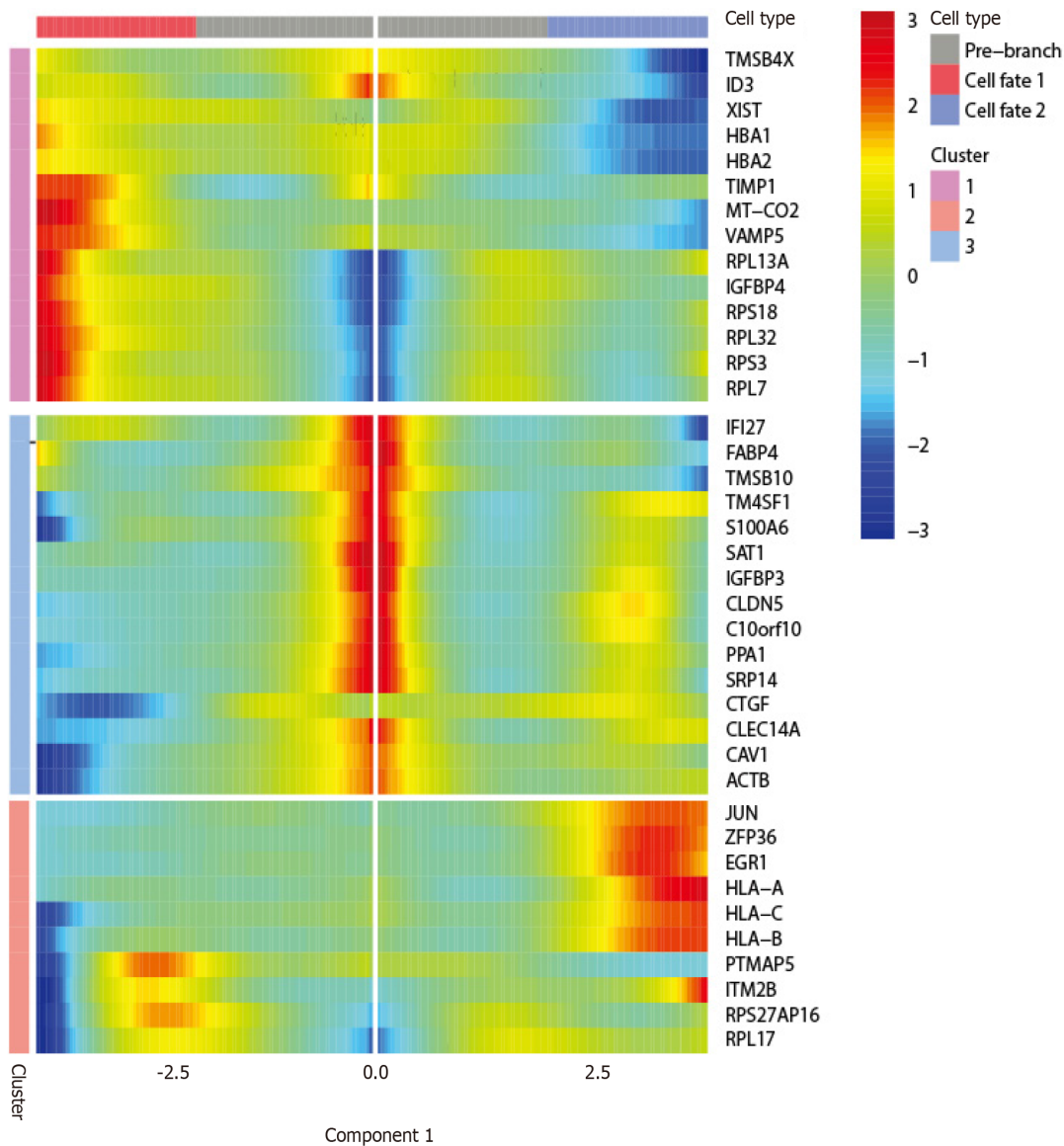
Analysis: The medium was changed to normal medium, and the experimental application phase of the Vorganoids experimental model was started (Figure 1). The standard experimental procedures for [5] identifying the organoids were performed according to previous methods.



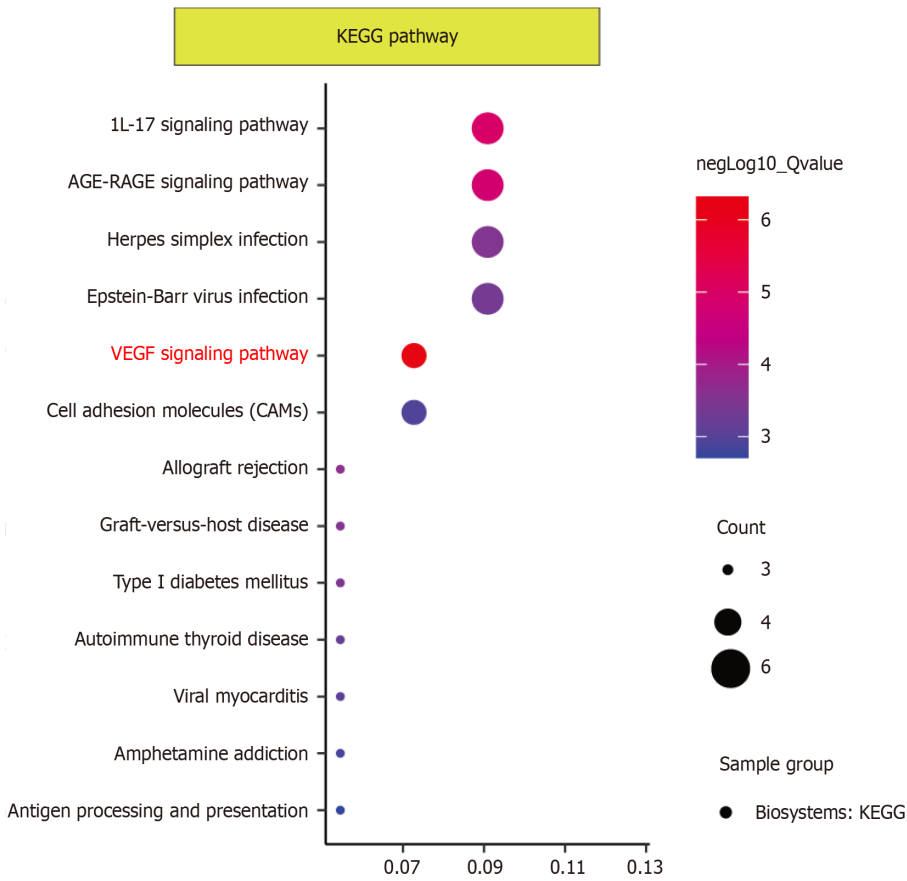
B



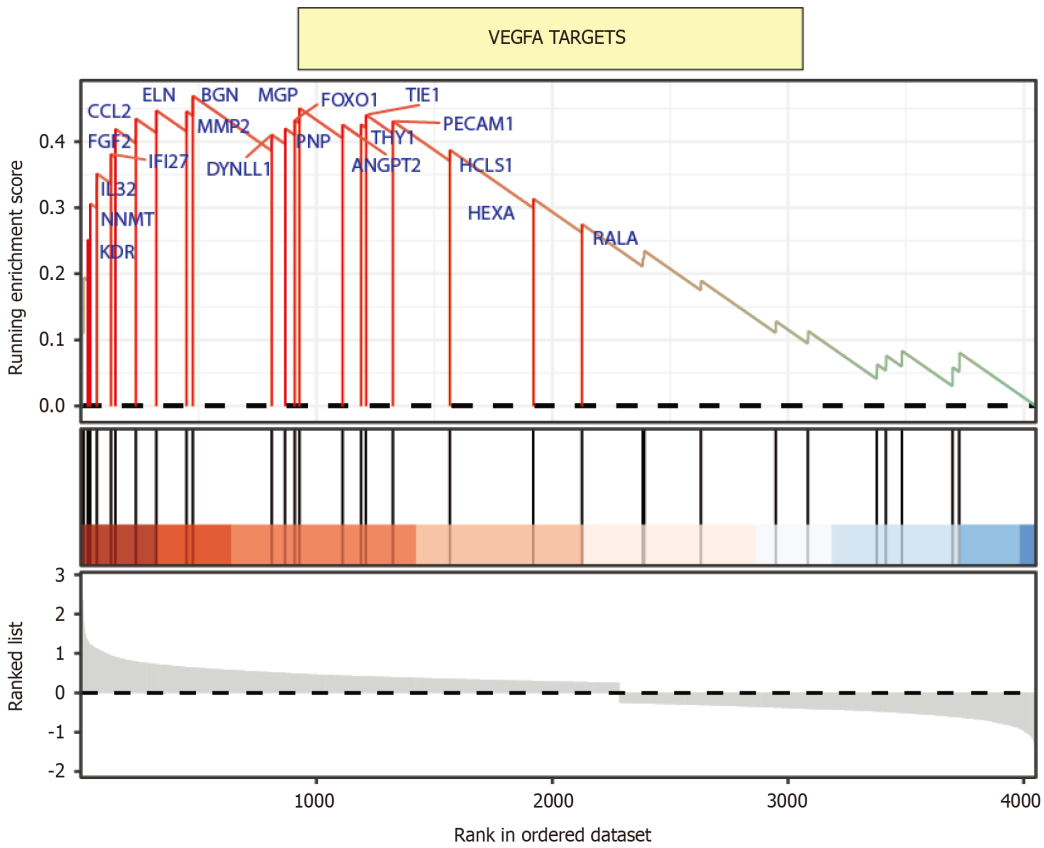
D



E



F



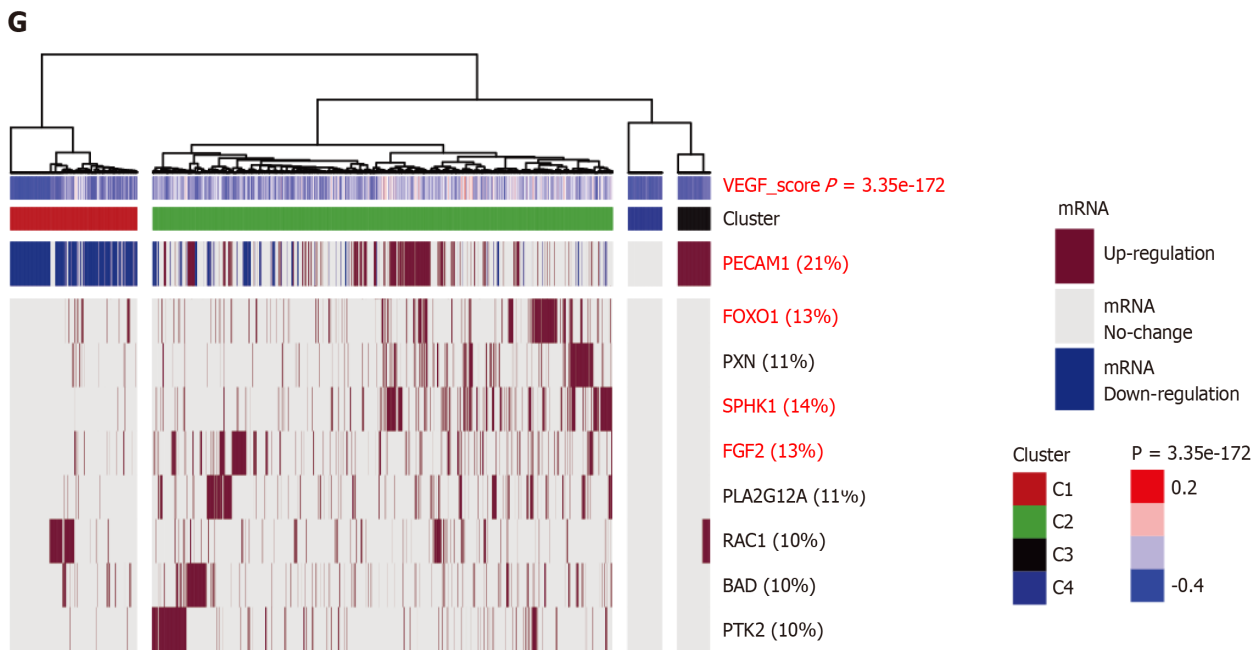


Figure 1 The single-cell atlas of human teeth. A: Single-cell RNA sequencing data from human teeth were projected onto the UMAP map. Annotation-cell and nonannotation clusters are presented on the same UMAP plot; B: The top 5 upregulated and downregulated differentially expressed genes (DEGs) were subsequently detected in each cell cluster; C: The UMAP map shows all the endothelial cell subsets; D: Heatmap of DEGs associated with endothelial cell subset development according to pseudotime trajectory analysis. The prebranch, cell fate1, and cell fate2 subsets of endothelial cells exhibit distinct fates; E: Vascular endothelial growth factor A targets identified by gene set enrichment analysis for pseudotime trajectory-related DEGs; F: GSVA and Ternary Cluster analyses revealed a significant difference in the vascular endothelial growth factor signalling pathway among the dental pulp endothelial cells; G: The GSVA and Ternary Cluster analyses showed a significant difference in vascular endothelial growth factor signaling pathway among dental pulp endothelial cells. VEGFA: Vascular endothelial growth factor A; IL: Interleukin; KEGG: Kyoto Encyclopedia of Genes and Genomes.

Hematoxylin-eosin staining

Various tissues were placed in 4% paraformaldehyde for histological examination. The tissues were dehydrated, embedded in paraffin, cut into 4 μm thick slices, and baked in an oven at 60 $^{\circ}\text{C}$ for 3 h. Paraffin was removed for hematoxylin-eosin (HE) staining, and the sections were observed and photographed under a microscope (Nikon, Tokyo, Japan).

Transmission electron microscopy imaging

For morphological analysis, the samples were then fixed with 2.5% glutaraldehyde for 12 h at room temperature. The samples were dehydrated in a graded series of ethanol (50%-100%), permeabilized with propylene oxide, and embedded in a poly/bed 812 kit (Polysciences, Washington, PA, United States). After embedding and polymerising the pure fresh resin in an electron microscope oven (DOSAKA) for 24 h, the initial sections were cut at approximately 50-200 nm, stained with toluidine blue (Sigma), and examined *via* light microscopy. Sections of approximately 70 nm were double stained with 6% uranyl acetate and lead citrate (Thermo Fisher Scientific, Waltham, MA, United States) for comparison. These sections were cut using a Leica EM UC-7 (Leica Microsystems, Tokyo, Japan) instrument equipped with a diamond knife (Diatome, Hatfield, PA, United States) and then transferred to copper and nickel grids. A transmission electron microscope (JEOL) with an acceleration voltage of 80 kV was used to observe all thin sections.

Immunofluorescence staining

Samples from each group were fixed with 4% paraformaldehyde for 24 h and subsequently incubated with 0.5% Triton-X for 10 min. Bovine serum albumin (1%) was used to block the cells for 1 h. Samples were dehydrated in sections after paraffin embedding. After blocking with 5% goat serum (Life Technologies, New York, NY, United States) for 1 h at 20 $^{\circ}\text{C}$, the specimens were then treated with rabbit anti-CD31 (Cell Signaling Technology, Boston, United States), anti-VE-cadherin (Cell Signaling Technology, Boston, United States), FGF2 (Ab208687-40, Abcam, Shanghai, United States), anti-FOXO1 (Cell Signaling Technology, Boston, United States), or anti-p-AKT (Cell Signaling Technology, Boston, United States) antibodies for 12 h at 4 $^{\circ}\text{C}$. Alexa Fluor 594-conjugated goat anti-rabbit secondary antibody (GB25303; Sevicebio, Wuhan, China) was added, and the cells were incubated for 2 h at room temperature. The nuclei were stained with 4',6-diamidino-2-phenylindole. CD31, VE-cadherin, FGF2, FOXO1, and p-AKT expression was observed under a fluorescence microscope (Nikon Eclipse, Tokyo, Japan). Statistical analysis was performed using GraphPad Prism 7 Software (San Diego, CA, United States).

Adenosine triphosphate

To quantify the metabolic activity of Vorganoids formed at different stages. RIPA buffer was added to lyse the

Vorganoids, which were subsequently centrifuged at 4 °C for 5 min at 12000 rpm, after which the supernatant was removed for adenosine triphosphate (ATP) determination. The ATP assay working solution was prepared according to the kit instructions (S0026, Beyotime, China), and an ATP standard curve was constructed. The ATP working solution (100 µL) was added to the test wells and allowed to stand for 3-5 min at room temperature to eliminate background effects. Then, an appropriate amount of sample or standard was added and mixed well. The relative light unit value was measured using a chemiluminescence metre.

Lactate dehydrogenase assay

To quantify the degree of cell death at VOrganoids that formed at different stages, the culture supernatants were changed to serum-free DMEM 24 h before the culture medium was aspirated from each well, and the sediment was removed by centrifugation at 1000 rpm for 5 min according to the manufacturer's protocol. A kit was used to measure the lactate dehydrogenase (LDH) concentration in each group of cultures according to the manufacturer's instructions (C0017, Beyotime, China).

Enzyme-linked immunosorbent assay

To quantify the expression of inflammatory markers in VOrganoids that formed at different stages, the levels of interleukin (IL)-6, IL-8, IL-10, IL-1β, and tumour necrosis factor-α in culture supernatants were assayed *via* enzyme-linked immunosorbent assay (BioLegend) according to the manufacturer's instructions.

Statistical analysis

The data were analysed using IBM SPSS Statistics 22.0 and Image-Pro Plus 6.0, and the normality and variance of the data distribution were analysed using the Kolmogorov-Smirnov test and Levene's test, respectively. Means were compared between two groups by *t* tests, and means were compared between multiple groups by one-way ANOVA with Bonferroni correction for two-way comparisons. Differences were considered statistically significant when $P < 0.05$.

RESULTS

scRNA-seq analysis

After quality control, we found no differences in the cell cycle distribution between the single-cell subpopulations. Cell clustering by UMAP resulted in 13 cell subpopulations in two spatial dimensions, which were annotated and divided into six classes: Chondrocytes, ECs, epithelial cells, neurons, natural killer cells, and tissue stem cells (Figure 1A). Among the DEGs, *FDCSP*, *KRT14*, *S100A8*, *S100A9*, and *S100A2* were the most common upregulated DEGs, while *COL3A1*, *COL1A2*, *IGFBP7*, *COL1A1*, and *VIM* were the most common. For ECs, the upregulated DEGs were *IFI27*, *ACKR1*, *RAMP2*, *AQP1*, and *GNG11*, and the downregulated DEGs were *S100A2*, *S100A9*, *KRT14*, and *S100A8*. For chondrocytes, *COL1A1*, *COL1A2*, *POSTN*, *ASPN*, and *COL3A1* were upregulated DEGs, while *S100A2*, *KRT14*, *S100A9*, and *S100A8* were downregulated DEGs (Figure 1B).

Reclustering analysis of core cell subpopulations

ECs were re-extracted and reclustered. The 2D cell distribution determined by UMAP was used to analyse the cell spatial clustering, and four subpopulations were obtained (Figure 1C). Pseudotime-series analysis revealed that the cell population could be divided into three developmental stages, and hub regulators are also presented (Figure 1D). GO analysis of development-related genes revealed that the primary regulatory pathways were closely related to ribonucleo-protein complex biogenesis, proteasomal protein catabolic process, and RNA splicing.

EC pseudotime series and functional enrichment analyses

Pseudotime-series analysis of ECs revealed that *CRIP1*, *IFITM1*, and *B2M* were expressed at high levels in fate2 ECs, while *TMSB4X*, *ID3*, and *XIST* were expressed at low levels. In fate1 cells, *MT-ND4*, *TIMP1*, and *MT-CO2* were highly expressed, while *PTMAP5*, *ITM2B*, and *RPS27AP16* were expressed at low levels. In differentiating cells, *MT-RNR1*, *MT-RNR2*, and *DNASE1L3* were expressed at low levels, while *IFI27*, *FABP4*, and *TMSB10* were highly expressed (Figure 1D). Kyoto Encyclopedia of Genes and Genomes pathway analysis revealed that the VEGF signalling pathway (B-H adjusted P value = 4.63E-06, gene count = 4), the IL-17 signalling pathway (B-H adjusted P value = 1.18E-05, gene count = 5), and the AGE-RAGE signalling pathway in diabetic complications (B-H adjusted P value = 1.60E-05, gene count = 5) were the predominant pathways enriched (Figure 1E).

GSEA of core pathways

GSEA showed that WESTON-VEGFA TARGETS (enrichment score = 0.47, normalised enrichment score = 2.11, and B-H adjusted P value = 0.018) was associated with endodontium differentiation and progression. *BGN*, *ELN*, *FOXO1*, *TIE1*, and *PECAM1*, which had relatively high running enrichment scores, were considered key regulators of dental pulp development (Figure 1F). In addition, GSEA and ternary cluster analyses revealed a significant difference in the VEGF signalling pathway among the dental pulp ECs ($P = 3.35e-172$). *PECAM1* (21%), *FGF2* (13%), *FOXO1* (13%), and *SPHK1* (14%) were the core genes with high variability (Figure 1G).

Derivation of human dental papilla cells from mesenchymal tissue with multipotential differentiation potential

To investigate the multidirectional differentiation potential of hDPSCs, we first established hDPSCs from pulp tissues extracted from third molars (patient age: 15 to 25 years). Cell surface marker identification experiments showed that the hDPSCs were derived from mesenchymal tissue and expressed mesenchymal-specific surface markers (Figure 2A). Multidirectional differentiation experiments revealed that hDPSCs could differentiate into osteogenic cells, cartilage cells, and adipocytes and express their corresponding specific markers (Figure 2B). Collectively, these data proved that hDPSCs exhibit multidirectional differentiation potential.

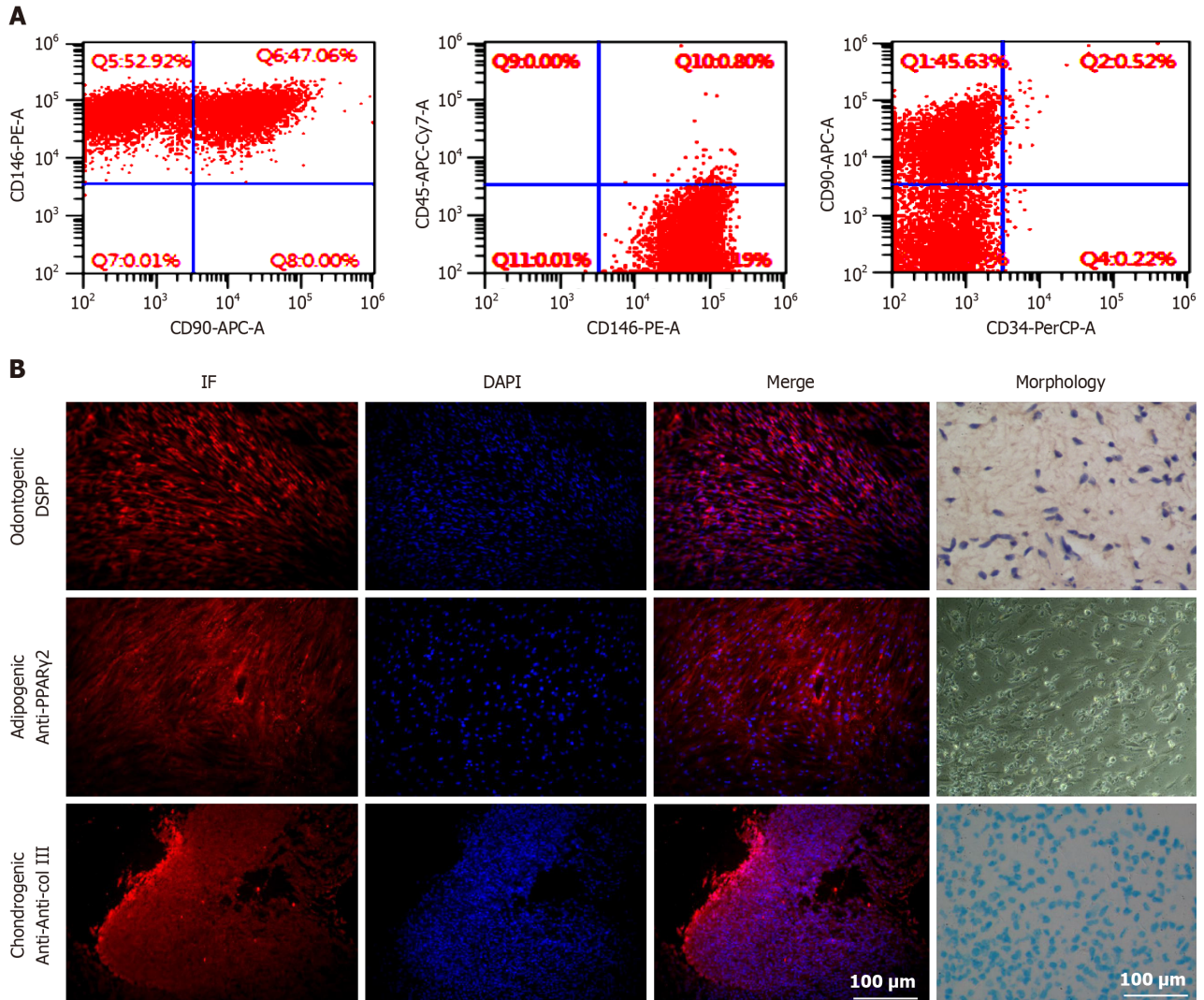


Figure 2 Human dental pulp stem cell culture and identification of multilineage differentiation ability. A: Human dental pulp stem cell surface marker identification; B: Immunofluorescence staining for dentin sialophosphoprotein, peroxisome proliferator-activated receptor γ 2, and collagen type III. Osteogenic, adipogenic, and chondrogenic differentiation were examined by assessing mineralised nodule formation, oil red O staining, and alcian blue staining, respectively, via pellet culture (morphology). Scale bar = 100 μ m. DSPP: Dentin sialophosphoprotein; PPAR γ 2: Peroxisome proliferator-activated receptor γ 2; col III: Collagen type III; IF: Immunofluorescence; DAPI: 4',6-diamidino-2-phenylindole.

Morphological and functional identification of vascularized human dental pulp organoids

The cells began to aggregate into clusters at approximately 6 h and formed a single spherical morphology after approximately 1 d. The final diameter of the Vorganoid was approximately 400-600 μ m. After the addition of 0.3% Triton X to permeabilize the Vorganoids for 30 min, the cells were unevenly distributed within the Vorganoids, and flocculent and irregularly distributed within the Vorganoids were observed. Long-term cultures of Vorganoids showed irregular cell proliferation and hyaline stroma at the edges, and Vorganoids were cultured continuously for more than 42 d *in vitro* (Figure 3A). HE staining and transmission electron microscopy revealed that the cells at the edge of the Vorganoids were arranged in a spindle row complex with normal intracellular organelles and fewer necrotic cells. In contrast, lysosome-like vesicles, which are polygonal in shape and tend to be compressed, appear in central cells. Compared to those in organoid culture, Vorganoids in culture had a greater proportion of Matrigel, a looser cell density and internal structure, fewer necrotic cells, and a greater distribution density and morphology similar to those of dental pulp tissue (Figure 3B).

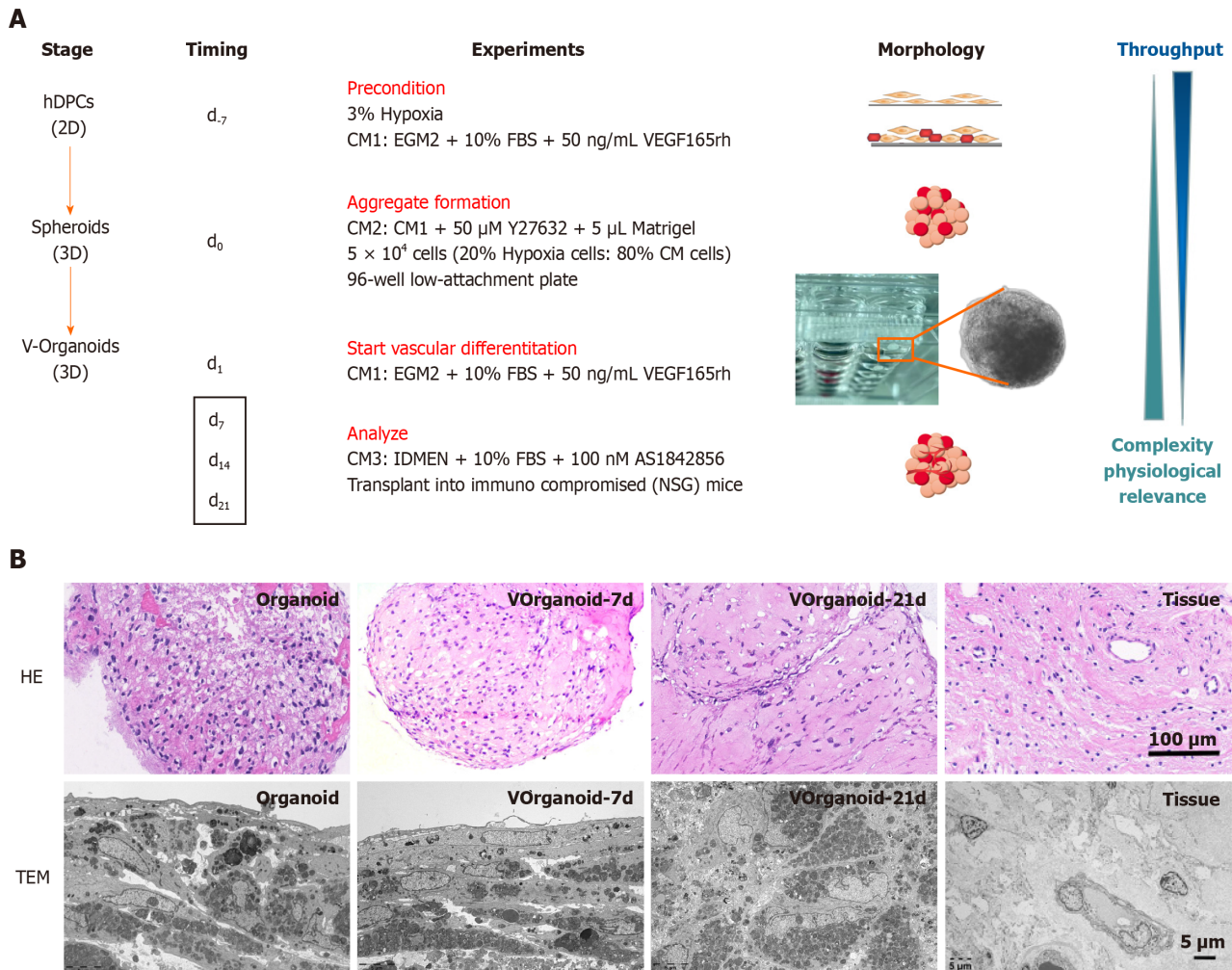


Figure 3 Strategies for the construction of a model for the study of prevascularized dental pulp organoids (Vorganoids). A: Schematic diagram of the timeline for generating Vorganoids from human dental pulp stem cells; B: Morphological differences between normal tissues, organoids, and vorganoids. Scale bar for hematoxylin-eosin staining = 100 μm and for transchromatic electron microscope = 5 μm. CM: Condition medium; HE: Hematoxylin-eosin; TEM: Transchromatic electron microscope; hDPCs: Human dental pulp stem cells; VEGF: Vascular endothelial growth factor; CM: Conditioned medium; FBS: Foetal bovine serum.

Differences in the expression of the angiogenic markers CD31 and VE were compared in three different tissues. CD31 was weakly expressed in pulp tissue, and VE was less expressed; CD31 was weakly expressed in organoids, while VE was not expressed; and the fluorescence intensities of CD31 and VE were greater in Vorganoid than in pulp tissue and organoids (Figure 4A). CD31 expression increased in the early stages of culture, reaching a peak at 14 d, with a subsequent decrease in expression (Figure 4B). The Vorganoids maintained a morphology similar to that of dental pulp for the first 21 d of *in vitro* culture, but when the culture time was extended to 28 d, loose dissociation occurred within the Vorganoid masses (Figure 4C). The ATP concentration decreased with increasing culture time, and the LDH concentration increased with increasing culture time (Figure 4D and E). The expression of IL-6 and IL-8 increased (Figure 4F), but there were no statistically significant differences in the expression of the other inflammatory factors. This finding suggested that the optimal period for using Vorganoids as a model for *in vitro* cell studies is within approximately 21 d.

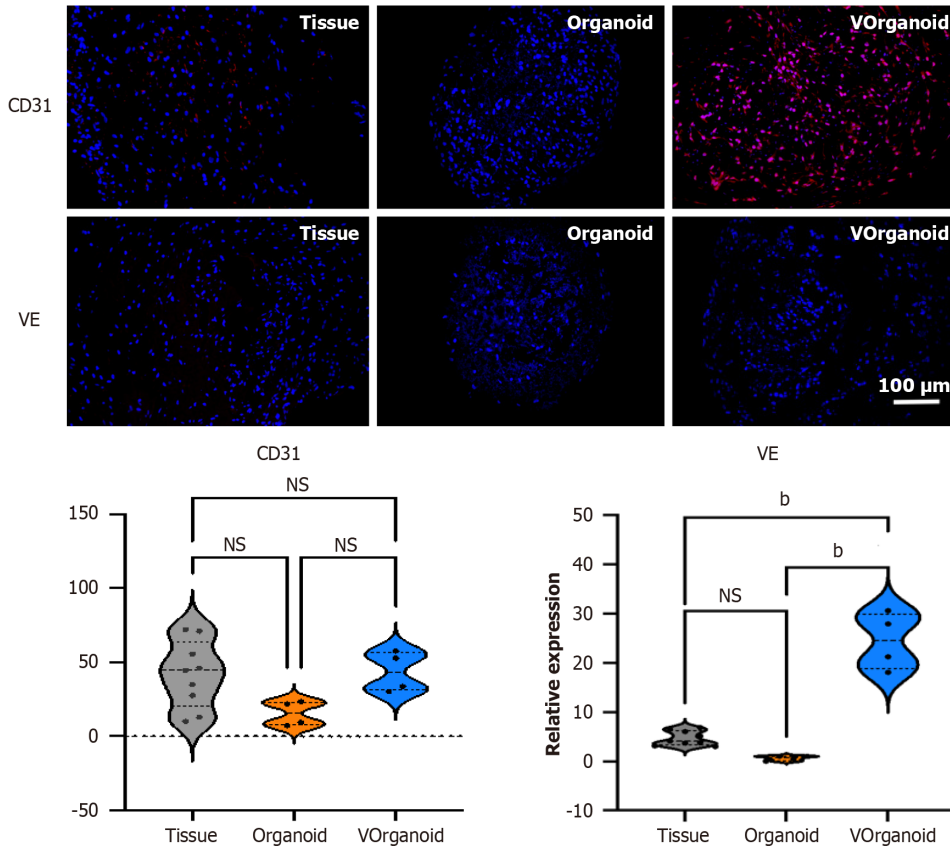
RNA-Seq analysis of dentin-pulp-like organoid development

By sample clustering analysis, we found that the pulp cells were well differentiated between the 2D/3D culture and normal groups (Figure 5A). Compared with control, organoid showed 4171 and 2598 up- and downregulated genes, respectively, and Vorganoid showed 5227 and 3355 up- and downregulated genes, respectively (Figure 5B and C). GSEA showed that the DEGs in the VEGFA pathway were significantly enriched in the organoid and Vorganoid groups relative to the control group (organoid *vs* control: Enrichment score = 0.61, NES = 1.22, *P*.adjust = 0.0082; Vorganoid *vs* control: Enrichment Score = 0.64, NES = 1.63, *P*.adjust = 0.0058) (Figure 5D and E).

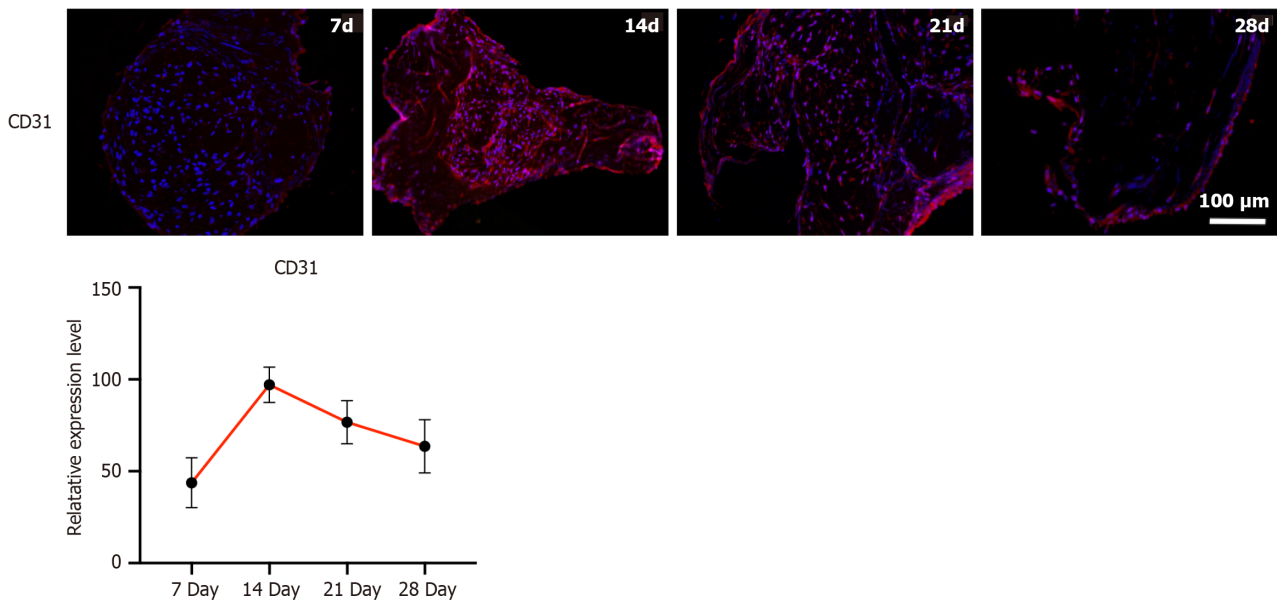
Target gene identification and validation

The above analyses revealed that the VEGFA TARGETS pathway may be the major pathway associated with the progression of and changes in the organoid and Vorganoid pathways compared to those in the control group. The enrich-

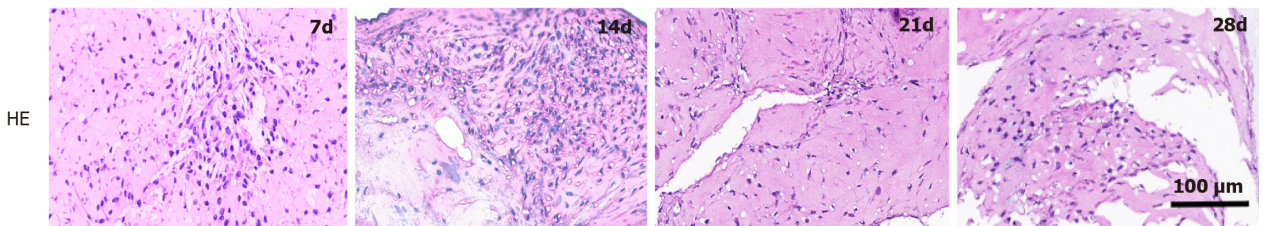
A



B



C



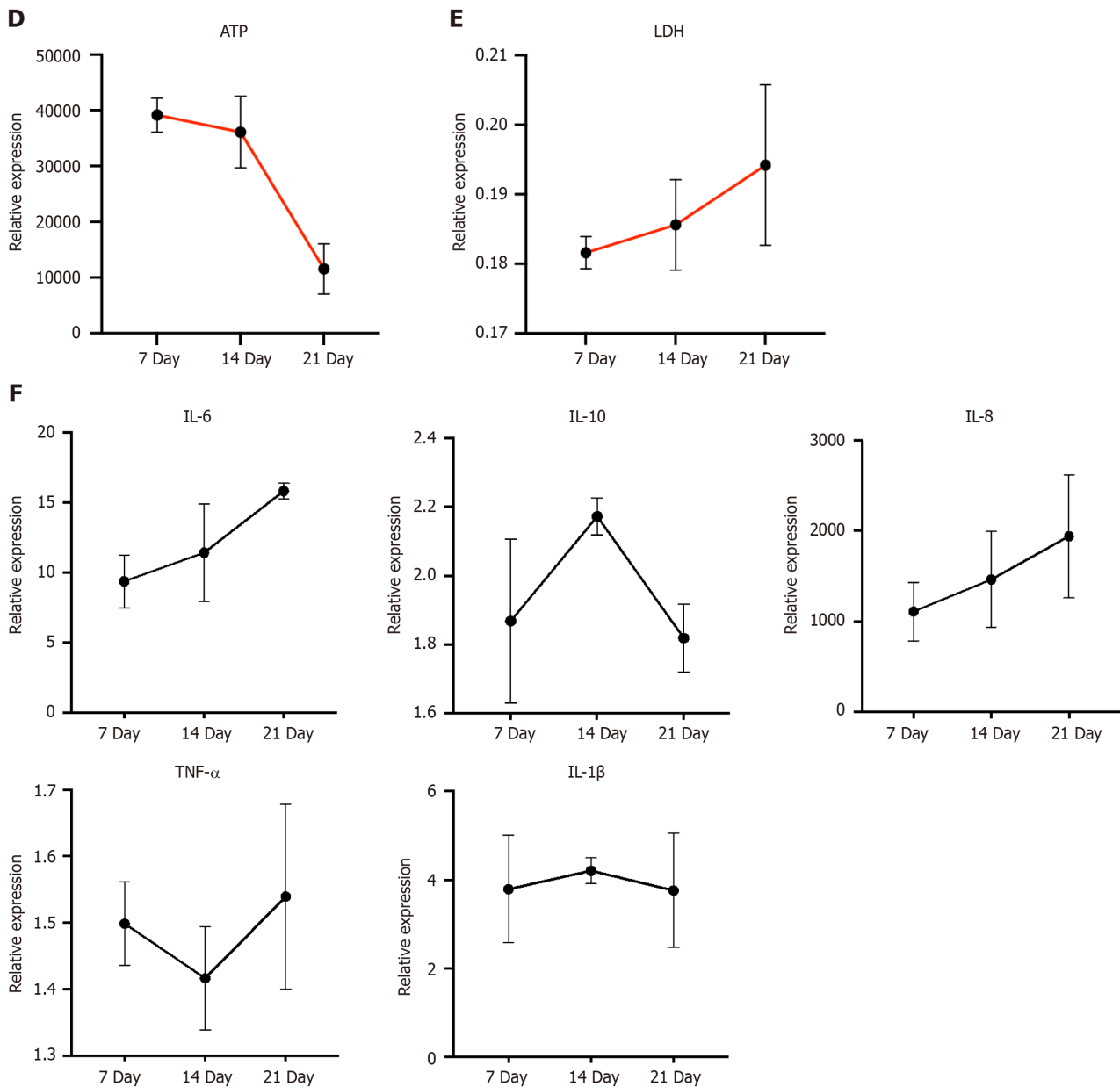


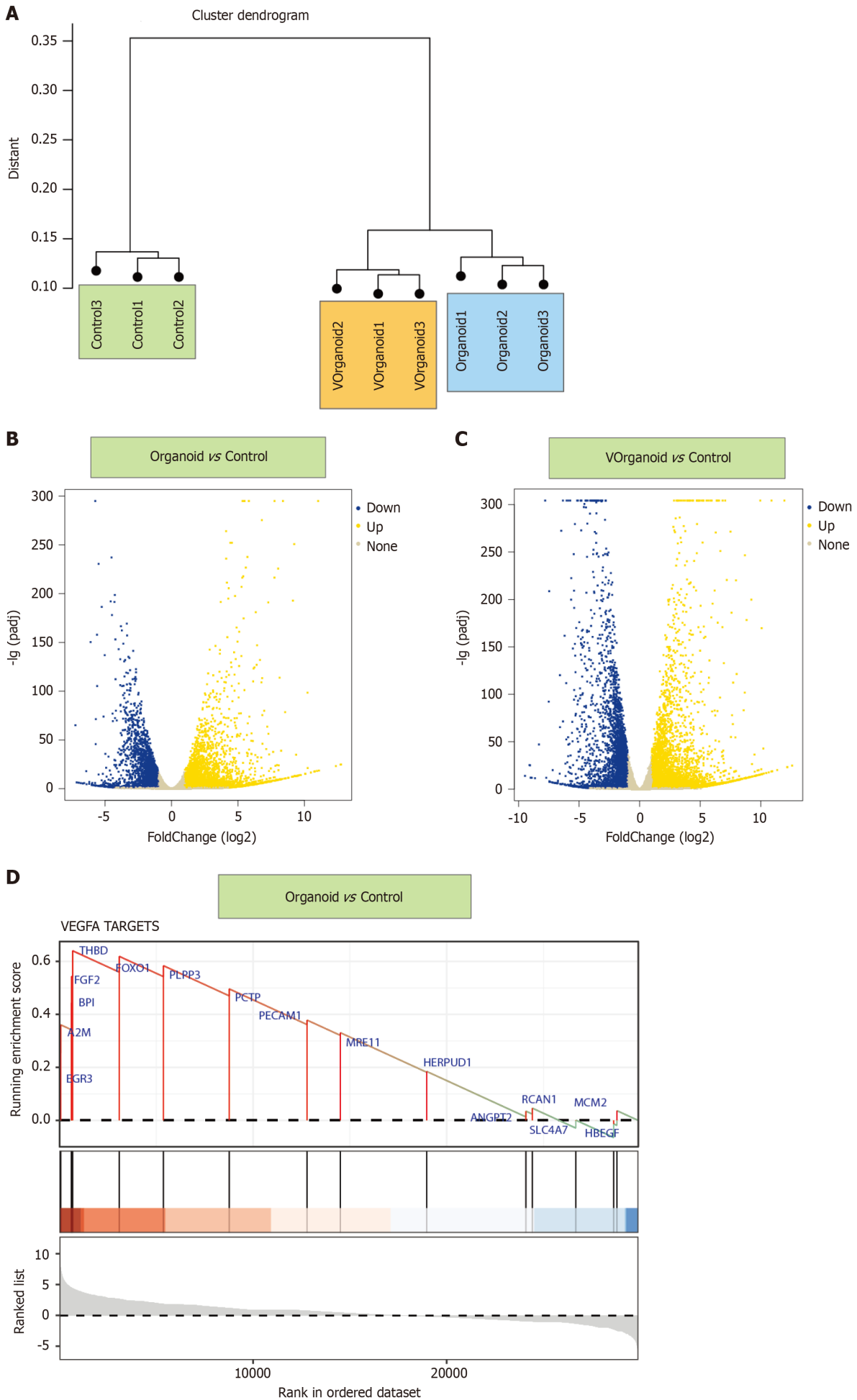
Figure 4 Morphological and functional identification of Vorganoids. A: Immunofluorescence staining for vasculogenesis-related markers; B: CD31 expression pattern in Vorganoid cells during different culture durations; C: Morphological changes in Vorganoid cells during different culture durations; D and E: Analysis of adenosine triphosphate (D) and lactate dehydrogenase (E) levels in Vorganoids during different culture durations; F: Expression patterns of inflammatory markers in Vorganoids analysed *via* enzyme-linked immunosorbent assay. Significant difference between the groups, ^b $P < 0.01$, Scale bar = 100 μm . HE: Hematoxylin-eosin; ATP: Adenosine triphosphate; LDH: Lactate dehydrogenase; IL: Interleukin; TNF: Tumour necrosis factor; NS: Not significant.

ment analysis revealed that the DEGs intersected with the DEGs identified by pseudotime series and single-cell RNA-seq analysis to identify three common DEGs: PECAM1 (21%), FGF2 (13%) and FOXO1 (13%) (Figure 5D).

Immunofluorescence staining revealed that the increase in FOXO1 and FGF2 expression was significantly greater in the Vorganoids group ($P < 0.05$) (Figure 6A). After 7 d of addition of the FOXO1 inhibitor AS1842856 to the Vorganoid medium, a decrease in CD31 expression and an increase in FGF2 expression were observed, as was a decrease in the ratio of p-AKT/FOXO1 expression, with no significant change in VE expression (Figure 6B).

DISCUSSION

Revascularization plays an important role in tissue engineering. In this study, first, prevascularized human pulp organoids were constructed, and the vascularized organoids were found to be more similar to normal pulp tissue in terms of function and morphology (Figure 7). hDPSCs have stem cell properties and can differentiate into different cell types for clinical restorative applications. High expression of CD105, CD133 and CD146 has been shown to indicate subpopulations of cells with high angiogenic potential[21]. Selected CD105-positive dental pulp cells encapsulated in collagen scaffolds



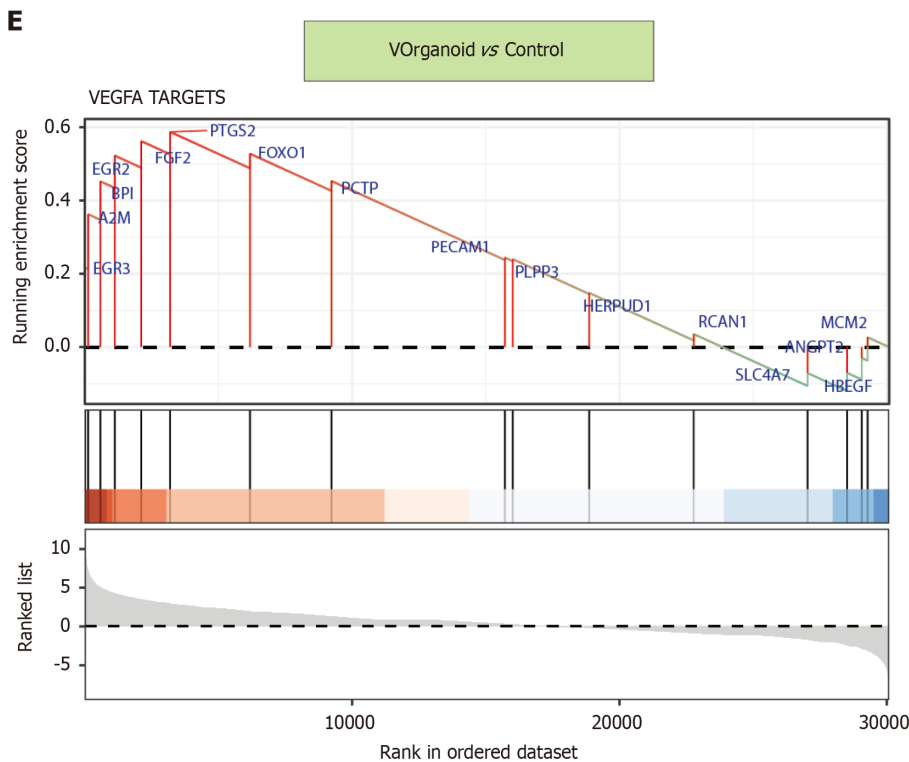


Figure 5 Functional enrichment analysis results for differentially expressed genes in the organoid vs control and Vorganoid vs control comparisons. A: The sample cluster dendrogram of different states of dentin-pulp-like organoid development; B and C: Volcano map showing the differentially expressed genes identified *via* differential comparison of the organoid vs control (B) and Vorganoid vs control (C) groups; D and E: The vascular endothelial growth factor A targets identified by gene set enrichment analysis enrichment analysis in the organoid vs control (D) and Vorganoid vs control (E) groups. VEGFA: Vascular endothelial growth factor A.

and stromal cell-derived factor 1 α and transplanted into root canals were able to form tissue with vascular-like structures [22]. In addition, the angiogenic capacities of different cell types differ; interactions between cells enhance angiogenic capacity, and an appropriate cell mixing ratio can significantly enhance angiogenesis[21,23-25]. In this study, the stemness of hDPSCs was maintained by 3% hypoxia treatment, vascularisation medium was added to promote the differentiation of pulp cells into ECs, Matrigel scaffolds provided attachment sites and growth space for the cells to maintain a suitable biomechanical microenvironment, and 3D coculture with unconditioned pulp cells was subsequently performed to promote organoid prevascularisation (Figures 5A and 7). Depending on the diffusional supply of nutrients and oxygen [26], the diameter of the Vorganoids remains within 500 μm . To promote organoid vascularisation, four elements, namely, cells, oxygen levels, scaffolding and signalling factors, work synergistically. The morphological and functional tests indicate that the Vorganoid partially. It should be noted that Vorganoids differ from tightly controlled structures *in vivo*. The use of *in vitro* models is limited in terms of representing the cell composition and structure of the *in vivo* counterpart, which can make them less reproducible.

To more thoroughly analyse the mechanisms involved in pulp tissue angiogenesis, we extracted single-cell sequencing data from public databases, further analysed the key regulatory pathways linking EC subpopulations in the tissue to angiogenesis, and performed a temporal analysis of key genes at different temporal and spatial nodes[27]. ECs were dominant in Vorganoid culture, and the proportion of ECs in the cell population was quite high in Vorganoid culture. Combined with the RNA-seq results, these findings revealed that the pathways associated with VEGFA targets were significantly enriched in the development of Vorganoids. Among the regulatory factors, the FOXO1 and FGF2 biomarkers were found to be involved in the regulation of Vorganoids.

FOXO1 is a key transcription factor involved in a wide range of biological functions. It is widely expressed in vascular ECs, and vascular cell adhesion molecule 1, intercellular adhesion molecule 1 and E-selectin have been reported to be downstream regulators of vascular ECs[28,29]. Systematic knockout of the *FOXO1* gene impaired angiogenesis and killed embryos, but specific knockout of the *FOXO1* gene in the adult mouse myocardium did not affect cardiac function[30,31]. Previous experiments showed that FOXO1 transcript expression was reduced in hypoxic culture but increased when the culture environment was changed to conditional induction culture or 3D organoid formation (Figure 7). Thus, FOXO1 may regulate different gene transcripts that act at different stages of angiogenesis, particularly during embryonic development. Therefore, we investigated the role of FOXO1 in the different stages of angiogenic differentiation in hDPSCs; however, it is unclear whether it plays a synergistic role between its antioxidant and angiogenic effects. This topic is worth investigating further.

The ability of cellular grafts to repair damaged tissues is limited, and the introduction of vascularized grafts brings them closer to the function and maturation of the corresponding tissues. This technique has the potential to overcome the limitations of many other models, such as maintaining *in vitro* accessibility and scalability, but significant improvements

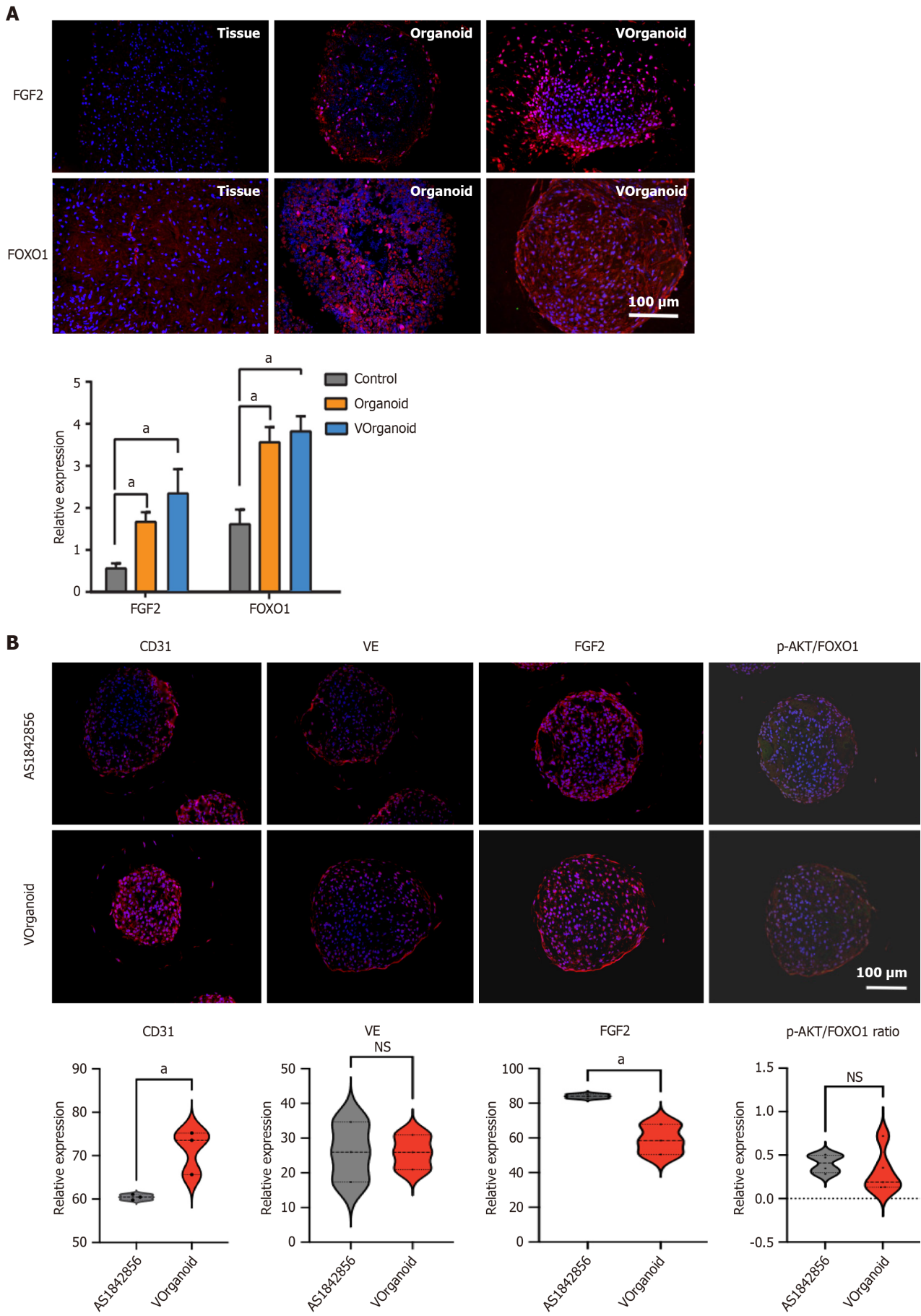


Figure 6 Target gene identification and validation. A and B: Immunofluorescence staining and quantification. Significant difference between the groups, ^aP < 0.05. Scale bar = 100 μ m. FGF2: Fibroblast growth factor 2; FOXO1: Forkhead box protein O1; NS: Not significant.

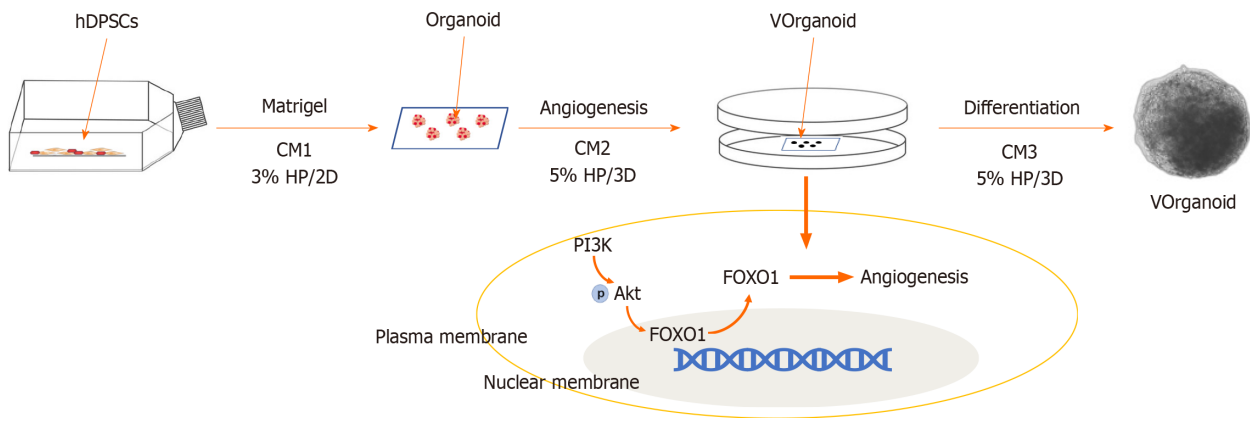


Figure 7 Generation of Vorganoids through differentiated human dental pulp stem cell assembly. hDPSCs: Human dental pulp stem cells; CM: Conditioned medium; FOXO1: Forkhead box protein O1.

are still needed. In conclusion, the finding of this study suggested that this new model could be applied in the field, which may pave the way for future dental regeneration prospects. In addition, vascularized organoids are more biologically similar to normal tissue. In addition to tissue regeneration and repair, Vorganoids can also be used for disease modelling, toxicity testing and drug screening. The use of human 3D organoids, along with other advances in single-cell technology, has revealed unprecedented insights into human biology and disease mechanisms.

CONCLUSION

Current organoid models do not fully replicate all cell types, levels of cell maturation, and physiological functions of their respective organs. They only exhibit some of the organ's functions. In this study, we effectively established an *in vitro* model of prevascularized dental pulp organoids and used it to elucidate new mechanisms of angiogenesis. Our results suggest that the biomarkers FOXO1 and FGF2 confirm the angiogenic regulatory role of Vorganoids. However, to understand the mechanisms by which organoids interact between structure and function, further investigation is required. Additionally, the use of organoids in simulating inflammation in clinically relevant diseases and the immunogenicity of dental materials should be studied.

ARTICLE HIGHLIGHTS

Research background

Stem cells can self-organise into micro-sized organ units, which can partially model tissue function and regeneration. Dental pulp organoids have been used to replicate the processes of tooth development and related diseases. However, the lack of vasculature limits the usefulness of dental pulp organoids.

Research motivation

The survival of stem cell transplants should be promoted, thereby improving the repair ability of the cells.

Research objectives

Three-dimensional (3D) self-assembly of a novel vascularised dental pulp-like organoid *in vitro* by hypoxia and conditioned media.

Research methods

Human dental pulp stem cells were induced from endothelial cells (ECs) through exposure to a hypoxic environment and conditioned medium. The resulting cells were then mixed with ECs at specific ratios and conditioned in a 3D environment to produce Vorganoids. The biological characteristics of the Vorganoids were analysed, and the regulatory pathways associated with angiogenesis were studied.

Research results

Vorganoids are similar in morphology and function to dental pulp tissue. Single-cell RNA sequencing of dental pulp tissue and RNA sequencing of Vorganoids were performed to identify the involvement of the biomarkers forkhead box protein O1 (FOXO1) and fibroblast growth factor 2 (FGF2) in key regulatory pathways associated with Vorganoid angiogenesis.

Research conclusions

In this study, we effectively established an *in vitro* model of prevascularized dental pulp organoids and used it to elucidate novel mechanisms of angiogenesis during dental regeneration. The biomarkers FOXO1 and FGF2 confirmed the angiogenesis-regulating role of angiopoietins.

Research perspectives

This innovative study has effectively established an *in vitro* model of prevascularized dental pulp organoids and used it to elucidate new mechanisms of angiogenesis during regeneration, facilitating the development of clinical treatment strategies.

FOOTNOTES

Co-first authors: Fei Liu and Jing Xiao.

Co-corresponding authors: Zhi-Ren Zhang and Chun-Xiao Bai.

Author contributions: Liu F, Xiao J, Tian JZ, Zhang ZR, and Bai XC designed the research; Liu F and Xiao J performed the research and analyzed the data; Chen LH and Pan YY contributed human dental pulp tissue; Liu F wrote the paper. Liu F and Xiao J contributed to the work equally and should be regarded as co-first authors. Bai XC and Zhang ZR contributed to the work equally and should be regarded as co-corresponding author.

Supported by the Science and Technology Programme of Guangzhou City, No. 202201020341.

Institutional review board statement: This study was approved by the Ethics Committee of Guangdong Second Provincial General Hospital.

Conflict-of-interest statement: All the authors report no relevant conflicts of interest for this article.

Data sharing statement: Technical appendix, statistical code, and dataset available from the corresponding author at kqliufei@126.com. Participants gave informed consent for data sharing.

Open-Access: This article is an open-access article that was selected by an in-house editor and fully peer-reviewed by external reviewers. It is distributed in accordance with the Creative Commons Attribution NonCommercial (CC BY-NC 4.0) license, which permits others to distribute, remix, adapt, build upon this work non-commercially, and license their derivative works on different terms, provided the original work is properly cited and the use is non-commercial. See: <https://creativecommons.org/licenses/by-nc/4.0/>

Country/Territory of origin: China

ORCID number: Fei Liu 0000-0002-5186-7661; Jun-Zhang Tian 0000-0002-4832-3648; Zhi-Ren Zhang 0000-0001-6780-4079; Xiao-Chun Bai 0000-0001-9631-4781.

S-Editor: Wang JJ

L-Editor: A

P-Editor: Zhao YQ

REFERENCES

- 1 **Roche ET**, Hastings CL, Lewin SA, Shvartsman D, Brudno Y, Vasilyev NV, O'Brien FJ, Walsh CJ, Duffy GP, Mooney DJ. Comparison of biomaterial delivery vehicles for improving acute retention of stem cells in the infarcted heart. *Biomaterials* 2014; **35**: 6850-6858 [PMID: 24862441 DOI: 10.1016/j.biomaterials.2014.04.114]
- 2 **Karp JM**, Leng Teo GS. Mesenchymal stem cell homing: the devil is in the details. *Cell Stem Cell* 2009; **4**: 206-216 [PMID: 19265660 DOI: 10.1016/j.stem.2009.02.001]
- 3 **Corsini NS**, Knoblich JA. Human organoids: New strategies and methods for analyzing human development and disease. *Cell* 2022; **185**: 2756-2769 [PMID: 35868278 DOI: 10.1016/j.cell.2022.06.051]
- 4 **Wimmer RA**, Leopoldi A, Aichinger M, Kerjaschki D, Penninger JM. Generation of blood vessel organoids from human pluripotent stem cells. *Nat Protoc* 2019; **14**: 3082-3100 [PMID: 31554955 DOI: 10.1038/s41596-019-0213-z]
- 5 **Jeong SY**, Lee S, Choi WH, Jee JH, Kim HR, Yoo J. Fabrication of Dentin-Pulp-Like Organoids Using Dental-Pulp Stem Cells. *Cells* 2020; **9**: [PMID: 32155898 DOI: 10.3390/cells9030642]
- 6 **Hemeryck L**, Hermans F, Chappell J, Kobayashi H, Lambrechts D, Lambrechts I, Bronckaers A, Vankelecom H. Organoids from human tooth showing epithelial stemness phenotype and differentiation potential. *Cell Mol Life Sci* 2022; **79**: 153 [PMID: 35217915 DOI: 10.1007/s00018-022-04183-8]
- 7 **Katata C**, Sasaki JI, Li A, Abe GL, Nör JE, Hayashi M, Imazato S. Fabrication of Vascularized DPSC Constructs for Efficient Pulp Regeneration. *J Dent Res* 2021; **100**: 1351-1358 [PMID: 33913364 DOI: 10.1177/00220345211007427]
- 8 **Stegen S**, van Gastel N, Eelen G, Ghesquière B, D'Anna F, Thienpont B, Goveia J, Torrekens S, Van Looveren R, Luyten FP, Maxwell PH, Wielockx B, Lambrechts D, Fendt SM, Carmeliet P, Carmeliet G. HIF-1 α Promotes Glutamine-Mediated Redox Homeostasis and Glycogen-

- Dependent Bioenergetics to Support Postimplantation Bone Cell Survival. *Cell Metab* 2016; **23**: 265-279 [PMID: 26863487 DOI: 10.1016/j.cmet.2016.01.002]
- 9 Bertassoni LE. Progress and Challenges in Microengineering the Dental Pulp Vascular Microenvironment. *J Endod* 2020; **46**: S90-S100 [PMID: 32950200 DOI: 10.1016/j.joen.2020.06.033]
 - 10 Carvalho GL, Sarra G, Schröter GT, Silva LSRG, Ariga SKK, Gonçalves F, Caballero-Flores HV, Moreira MS. Pro-angiogenic potential of a functionalized hydrogel scaffold as a secretome delivery platform: An innovative strategy for cell homing-based dental pulp tissue engineering. *J Tissue Eng Regen Med* 2022; **16**: 472-483 [PMID: 35244346 DOI: 10.1002/term.3294]
 - 11 Liu F, Huang X, Luo Z, He J, Haider F, Song C, Peng L, Chen T, Wu B. Hypoxia-Activated PI3K/Akt Inhibits Oxidative Stress via the Regulation of Reactive Oxygen Species in Human Dental Pulp Cells. *Oxid Med Cell Longev* 2019; **2019**: 6595189 [PMID: 30728888 DOI: 10.1155/2019/6595189]
 - 12 Clough E, Barrett T. The Gene Expression Omnibus Database. *Methods Mol Biol* 2016; **1418**: 93-110 [PMID: 27008011 DOI: 10.1007/978-1-4939-3578-9_5]
 - 13 Hafemeister C, Satija R. Normalization and variance stabilization of single-cell RNA-seq data using regularized negative binomial regression. *Genome Biol* 2019; **20**: 296 [PMID: 31870423 DOI: 10.1186/s13059-019-1874-1]
 - 14 Butler A, Hoffman P, Smibert P, Papalexi E, Satija R. Integrating single-cell transcriptomic data across different conditions, technologies, and species. *Nat Biotechnol* 2018; **36**: 411-420 [PMID: 29608179 DOI: 10.1038/nbt.4096]
 - 15 Sinha D, Sinha P, Saha R, Bandyopadhyay S, Sengupta D. Improved dropClust R package with integrative analysis support for scRNA-seq data. *Bioinformatics* 2019 [PMID: 31693086 DOI: 10.1093/bioinformatics/btz823]
 - 16 Slovin S, Carissimo A, Panariello F, Grimaldi A, Bouché V, Gambardella G, Cacchiarelli D. Single-Cell RNA Sequencing Analysis: A Step-by-Step Overview. *Methods Mol Biol* 2021; **2284**: 343-365 [PMID: 33835452 DOI: 10.1007/978-1-0716-1307-8_19]
 - 17 Wu T, Hu E, Xu S, Chen M, Guo P, Dai Z, Feng T, Zhou L, Tang W, Zhan L, Fu X, Liu S, Bo X, Yu G. clusterProfiler 4.0: A universal enrichment tool for interpreting omics data. *Innovation (Camb)* 2021; **2**: 100141 [PMID: 34557778 DOI: 10.1016/j.xinn.2021.100141]
 - 18 Hänzelmann S, Castelo R, Guinney J. GSEA: gene set variation analysis for microarray and RNA-seq data. *BMC Bioinformatics* 2013; **14**: 7 [PMID: 23323831 DOI: 10.1186/1471-2105-14-7]
 - 19 Anders S, Huber W. Differential expression analysis for sequence count data. *Genome Biol* 2010; **11**: R106 [PMID: 20979621 DOI: 10.1186/gb-2010-11-10-r106]
 - 20 Chen J, Bardes EE, Aronow BJ, Jegga AG. ToppGene Suite for gene list enrichment analysis and candidate gene prioritization. *Nucleic Acids Res* 2009; **37**: W305-W311 [PMID: 19465376 DOI: 10.1093/nar/gkp427]
 - 21 Gandia C, Armiñan A, García-Verdugo JM, Lledó E, Ruiz A, Miñana MD, Sanchez-Torrijos J, Payá R, Mirabet V, Carbonell-Uberos F, Llop M, Montero JA, Sepúlveda P. Human dental pulp stem cells improve left ventricular function, induce angiogenesis, and reduce infarct size in rats with acute myocardial infarction. *Stem Cells* 2008; **26**: 638-645 [PMID: 18079433 DOI: 10.1634/stemcells.2007-0484]
 - 22 Iohara K, Imabayashi K, Ishizaka R, Watanabe A, Nabekura J, Ito M, Matsushita K, Nakamura H, Nakashima M. Complete pulp regeneration after pulpectomy by transplantation of CD105+ stem cells with stromal cell-derived factor-1. *Tissue Eng Part A* 2011; **17**: 1911-1920 [PMID: 21417716 DOI: 10.1089/ten.TEA.2010.0615]
 - 23 Dissanayaka WL, Zhan X, Zhang C, Hargreaves KM, Jin L, Tong EH. Coculture of dental pulp stem cells with endothelial cells enhances osteo-/odontogenic and angiogenic potential in vitro. *J Endod* 2012; **38**: 454-463 [PMID: 22414829 DOI: 10.1016/j.joen.2011.12.024]
 - 24 Dissanayaka WL, Hargreaves KM, Jin L, Samaranyake LP, Zhang C. The interplay of dental pulp stem cells and endothelial cells in an injectable peptide hydrogel on angiogenesis and pulp regeneration in vivo. *Tissue Eng Part A* 2015; **21**: 550-563 [PMID: 25203774 DOI: 10.1089/ten.TEA.2014.0154]
 - 25 Xu X, Li Z, Ai X, Tang Y, Yang D, Dou L. Human three-dimensional dental pulp organoid model for toxicity screening of dental materials on dental pulp cells and tissue. *Int Endod J* 2022; **55**: 79-88 [PMID: 34587308 DOI: 10.1111/iej.13641]
 - 26 Wörsdörfer P, Ergün S. The Impact of Oxygen Availability and Multilineage Communication on Organoid Maturation. *Antioxid Redox Signal* 2021; **35**: 217-233 [PMID: 33334234 DOI: 10.1089/ars.2020.8195]
 - 27 Vargas-Valderrama A, Messina A, Mitjavila-Garcia MT, Guenou H. The endothelium, a key actor in organ development and hPSC-derived organoid vascularization. *J Biomed Sci* 2020; **27**: 67 [PMID: 32443983 DOI: 10.1186/s12929-020-00661-y]
 - 28 Wang S, Shi M, Li J, Zhang Y, Wang W, Xu P, Li Y. Endothelial cell-derived exosomal circHIPK3 promotes the proliferation of vascular smooth muscle cells induced by high glucose via the miR-106a-5p/Foxo1/Vcam1 pathway. *Aging (Albany NY)* 2021; **13**: 25241-25255 [PMID: 34887361 DOI: 10.18632/aging.203742]
 - 29 Zhuang T, Liu J, Chen X, Zhang L, Pi J, Sun H, Li L, Bauer R, Wang H, Yu Z, Zhang Q, Tomlinson B, Chan P, Zheng X, Morrissey E, Liu Z, Reilly M, Zhang Y. Endothelial Foxp1 Suppresses Atherosclerosis via Modulation of Nlrp3 Inflammasome Activation. *Circ Res* 2019; **125**: 590-605 [PMID: 31318658 DOI: 10.1161/CIRCRESAHA.118.314402]
 - 30 Hariharan N, Maejima Y, Nakae J, Paik J, Depinho RA, Sadoshima J. Deacetylation of FoxO by Sirt1 Plays an Essential Role in Mediating Starvation-Induced Autophagy in Cardiac Myocytes. *Circ Res* 2010; **107**: 1470-1482 [PMID: 20947830 DOI: 10.1161/CIRCRESAHA.110.227371]
 - 31 Qi Y, Zhu Q, Zhang K, Thomas C, Wu Y, Kumar R, Baker KM, Xu Z, Chen S, Guo S. Activation of Foxo1 by insulin resistance promotes cardiac dysfunction and β -myosin heavy chain gene expression. *Circ Heart Fail* 2015; **8**: 198-208 [PMID: 25477432 DOI: 10.1161/CIRCHEARTFAILURE.114.001457]



Published by **Baishideng Publishing Group Inc**
7041 Koll Center Parkway, Suite 160, Pleasanton, CA 94566, USA
Telephone: +1-925-3991568
E-mail: office@baishideng.com
Help Desk: <https://www.f6publishing.com/helpdesk>
<https://www.wjgnet.com>

